

Effective fast electron acceleration along the target surface

X. H. Yuan^{1,2}, Y.T Li^{1,*}, M. H. Xu¹, Z. Y. Zheng¹, Q. Z. Yu¹, W. X. Liang¹, Y. Zhang¹,
F. Liu¹, Jens Bernhardt¹, S. J. Wang¹, Z. H. Wang¹, W. J. Ling¹,
Z. Y. Wei¹, W. Zhao², J. Zhang^{1,3,*}

¹Beijing National Laboratory for Condensed Matter Physics, Institute of Physics, Chinese Academy of Sciences, Beijing 100080

²State Key Laboratory of Transient Optics and Photonics, Xi'an Institute of Optics and Precision Mechanics, Chinese Academy of Sciences, Xi'an 710119

³Department of Physics, Shanghai Jiao Tong University, Shanghai 200240

*Corresponding author: jzhang@aphy.iphy.ac.cn, ytli@aphy.iphy.ac.cn

Abstract: The dependence of angular distributions of fast electrons generated in the interaction of p-polarized femtosecond laser pulses with foil targets on laser intensities is investigated. A novel fast electron beam along the front target surface is observed for high laser intensity. It is found that the electron acceleration along the target surface is more efficient than those in other directions.

©2008 Optical Society of America

OCIS codes: (020.2649) strong field laser physics; (350.3390) Laser materials processing; (350.5400) Plasmas

References and links

1. M. Tabak, J. Hammer, M. E. Glinsky, W. L. Kruer, S.C.Wilks, J. Woodworth, E. M. Campbell, and M. D. Perry, "Ignition and high gain with ultrapowerful lasers," *Phys. Plasmas* **1**, 1626-1634 (1994).
2. H. Schwoerer, S. Pfotenhauer, O. Jackel, K.-U. Amthor, B. Liesfeld, W. Ziegler, R. Sauerbrey, T. Esirkepov and K. W. D. Ledingham, "Laser-plasma acceleration of quasi-monoenergetic protons from microstructured targets," *Nature* **439**, 445-448 (2006).
3. G. Pretzler, F. Brandl, J. Stein, E. Fill and J. Kuba, "High-intensity regime of x-ray generation from relativistic laser plasmas," *Appl. Phys. Lett.* **82**, 3623-3625 (2003).
4. S. Bastiani, P. Audebert, J. P. Geindre, Th. Schlegel, J. C. Gauthier, C. Quiox, G. Hamoniaux, G. Grillon, and A. Antonetti, "Hot-electron distribution functions in a subpicosecond laser interaction with solid targets of varying initial gradient scale lengths," *Phys. Rev. E* **60**, 3439-3452 (1999).
5. Y. Y. Ma, Z. M. Sheng, Y. T. Li, J. Zhang, X. H. Yuan, M. H. Xu, Z. Y. Zheng, W. W. Chang, M. Chen and J. Zheng, "Preplasma effects on the emission directions of energetic electrons in relativistic laser-solid interactions," *J. Plasma Phys.* **72**, 1269-1272 (2006).
6. F. N. Beg, E. L. Clark, M. S. Wei, A. E. Dangor, R.G. Evans, A. Gopal, K. L. Lancaster, K.W. D. Ledingham, P. McKenna, P. A. Norreys, M. Tatarakis, M. Zepf and K. Krushelnick, "High-Intensity-Laser-Driven Z Pinche," *Phys. Rev. Lett.* **92**, 95001-95004 (2004).
7. Y. T. Li, J. Zhang, Z. M. Sheng, H. Teng, T. J. Liang, X. Y. Peng, X. Lu, Y. J. Li and X. W. Tang, "Spatial Distribution of High-Energy Electron Emission from Water Plasmas Produced by Femtosecond Laser Pulses," *Phys. Rev. Lett.* **90**, 165002-165005 (2003).
8. Z. L. Chen, R. Kodama, M. Nakatsutsumi, H. Nakamura, M. Tampo, K. A. Tanaka, Y. Toyama, T. Tsutsumi, and T. Yabuuchi, "Enhancement of energetic electrons and protons by cone guiding of laser light," *Phys. Rev. E* **71**, 36403-36407 (2005).
9. Y. T. Li, J. Zhang, Z. M. Sheng, J. Zheng, Z. L. Chen, R. Kodama, T. Matsuoka, M. Tampo, K. A. Tanaka, T. Tsutsumi and T. Yabuuchi, "High-energy electrons produced in subpicosecond laser-plasma interactions from subrelativistic laser intensities to relativistic intensities," *Phys. Rev. E* **69**, 36405-36411 (2004).
10. A. G. Zhidkov, A. Sasaki, I. Fukumoto, T. Tajima, T. Auguste, P. D'Oliveira, S. Hulin, P. Monot, T. Auguste, P. D'Oliveira, S. Hulin, and P. Monot, "Pulse duration effect on the distribution of energetic particles produced by intense femtosecond laser pulses irradiating solids," *Phys. Plasmas* **8**, 3718-3723 (2001).
11. L. M. Chen, J. Zhang, Y. T. Li, H. Teng, T. J. Liang, Z. M. Sheng, Q. L. Dong, L. Z. Zhao, Z.Y. Wei, and X.W. Tang, "Effects of Laser Polarization on Jet Emission of Fast Electrons in Femtosecond-Laser Plasmas," *Phys. Rev. Lett.* **87**, 225001-225004 (2001).

12. S. Kato, E. Miura, E. Takahashi, T. Nakamura, T. Kato and Y. Owadano, "Effects of laser wavelength and density scalelength on absorption of ultrashort intense lasers on solid-density targets," *J. Plasma Fusion Res.* **78**, 717-718 (2002).
13. S. C. Wiks and W. L. Kruer, "Ultra-intense laser light by solids and overdense plasmas," *IEEE J. Quantum Electron.* **QE33**, 1954-1968 (1997).
14. F. Brunel, "Not-so-resonant, resonant absorption," *Phys. Rev. Lett.* **59**, 52-55 (1987).
15. W. L. Kruer and Estabrook, "JxB heating by very intense laser," *Phys. Fluids.* **28**, 430-432 (1985).
16. T. Nakamura, S. Kato, H. Nagatomo and K. Mima, "Surface-Magnetic-Field and Fast-Electron Current-Layer Formation by Ultraintense Laser Irradiation," *Phys. Rev. Lett.* **93**, 265002-265005 (2004).
17. Y. Sentoku, K. Mima, H. Ruhl, Y. Toyama, R. Kodama, T. E. Cowan, "Laser light and hot electron micro focusing using a conical target," *Phys. Plasmas* **11**, 3083-3087 (2004).
18. Y. T. Li, X. H. Yuan, M. H. Xu, Z.Y. Zheng, Z. M. Sheng, M. Chen, Y. Y. Ma, W. X. Liang, Q. Z. Yu, Y. Zhang, F. Liu, Z. H. Wang, Z.Y. Wei, W. Zhao, Z. Jin and J. Zhang, "Observation of a Fast Electron Beam Emitted along the Surface of a Target Irradiated by Intense Femtosecond Laser Pulses," *Phys. Rev. Lett.* **96**, 165003-165006 (2006).
19. M. Chen, Z. M. Sheng and J. Zhang, "On the angular distribution of fast electrons generated in intense laser interaction with solid targets," *Phys. Plasmas* **13**, 014504-014507 (2006).
20. M. Chen, Z. M. Sheng, I. Zheng, Y. Y. Ma, M. A. Bari, Y. T. Li and J. Zhang, "Surface electron acceleration in relativistic laser-solid interactions," *Optics Express* **14**, 3093-3098 (2006).
21. T. Nakamura, K. Mima, H. Sakagami, and T. Johzaki, "Electron surface acceleration on a solid capillary target inner wall irradiated with ultraintense laser pulses," *Phys. Plasmas* **14**, 053112-53118 (2007).

1. Introduction

The generation and transport of fast electrons in the interaction of short-pulse high-intensity lasers with targets have been widely investigated because of their potential applications [1-3]. It is found that the fast electron emission is strongly dependent on the parameters of plasmas [4-5], targets [6-8] and laser pulses [9-12]. Directional fast electron beams can be generated by different mechanisms. Resonant absorption [13] and vacuum heating [14] generate fast electrons in the normal direction of the target surface, while the $J \times B$ heating [15], wake field, etc., accelerate fast electrons mainly along the laser propagation direction. Recently a theory proposed by Nakamura *et al.* [16] and a PIC simulation done by Sentoku *et al.* [17] have predicted a fast electron beam along the target surface due to the quasistatic magnetic field. The predictions have been confirmed by our recent experiments [18], and supported by our analytic formula [19]. The generation of this novel emission can be schematically explained as follows: parts of fast electrons generated by the $J \times B$ or vacuum heating could be reflected to the vacuum by the quasistatic magnetic field. However, the electrostatic field in the vacuum will push them back into target again. The push-pull processes lead to the fast electron emission along the surface.

In this paper, we investigate experimentally the effects of the laser intensity on the fast electron emission along the front target surface by measuring the angular distribution of the fast electrons. Our results show that collimated beam of fast electrons appears only for higher intensities ($I > 7 \times 10^{17} \text{ W/cm}^2$). The electron count, relative fraction and temperature of the fast electrons increase with the laser intensity. This indicates that the electron acceleration along the front target surface is more effective at higher laser intensities than that in the other directions.

2. Experiment

The experiments were performed with the home-made Ti: sapphire laser system Xtreme Light II (XL-II) at the Institute of Physics, Chinese Academy of Sciences. This system is capable of delivering energies of up to 640 mJ with a repetition rate of 10 Hz. The pulse duration is 30 fs and central wavelength 800 nm. The p-polarized laser beam was focused onto an Al target of 30 μm thickness with an f/3.5 off-axis parabolic mirror. The incidence angle was 45° to the target normal. The focal spot was about 10 μm full width at half maximum (FWHM). The laser intensity on the target was adjusted between $6 \times 10^{16} \text{ W/cm}^2$ and $3 \times 10^{18} \text{ W/cm}^2$.

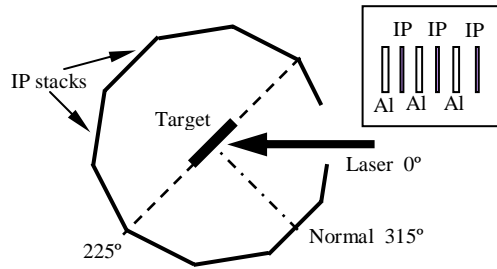


Fig. 1. Experimental setup.

Figure 1 shows the experimental setup. The spatial distribution of fast electrons was measured by an image plate (IP) stack detector. This detector consists of three layers of IPs. Al foils of selected thickness were inserted between each IP layer and also in front of the first layer for the energy-resolved measurement, as shown in the inset of Fig. 1. A layer of Al foil of 70 μm thickness was used to wrap the detector to stop the protons, energetic heavy ions, scattered laser light and electrons with energies lower than 120 keV. The distance from the laser focus to the stack was 55 mm. This detector can cover almost all 360 $^\circ$ angle range in the incident plane except for an open angle of 20 $^\circ$ left for laser entrance, and $\pm 27^\circ$ in the plane vertical to the incident plane. To make sure the signal was due to the electrons, null test by adding a 2000 Gaussian magnetic field before the IP was made, which gave a two-order decrease in the recorded signal.

3. Results and discussion

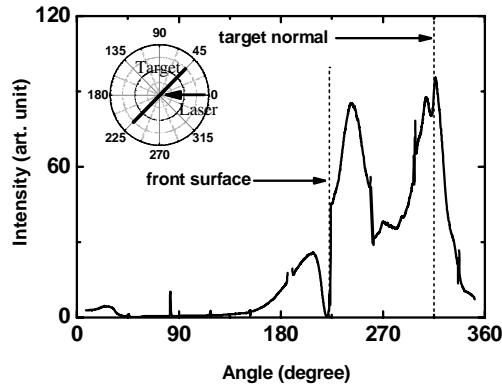


Fig. 2. Typical angular distribution of the fast electrons with energies larger than 550 keV for the laser intensity of $1.5 \times 10^{18} \text{ W/cm}^2$.

Figure 2 shows a typical angular distribution of the fast electrons with energies larger than 550 keV at a laser intensity of $1.5 \times 10^{18} \text{ W/cm}^2$ for the incidence angle 45 $^\circ$. The data are obtained by integrating the signal in the vertical direction. 0 $^\circ$ corresponds to the laser incidence direction. The fast electrons are mainly emitted along two directions. One is close to the target normal direction with a cone angle of about 32 $^\circ$ (FWHM). The other peaks at 17 $^\circ$ from the front target surface with a cone angle of about 36 $^\circ$ (FWHM). Note that there is also a small peak close to the surface behind the target. These characteristics are similar for electrons with different energies. The fast electron emission along the target surface for larger incidence

angles and the dependence on the electron density scale length of preplamas has been reported [18]. In the following we will concentrate on the dependence of the fast electrons close to the target surface on the laser intensities.

The laser intensities on targets were changed by adjusting the laser pulse energy. Figure 3 shows the angular distributions of the fast electrons with energies larger than 550 keV at four different laser intensities. The data have been rescaled to 100 for the maximum. All fast electrons are emitted close to the target normal direction at 6×10^{16} W/cm². However, more and more electrons are emitted nearly close to the target surface as laser intensities are increased. One can see that a small fraction of such fast electrons are presented at 7×10^{17} W/cm², while such electrons have dominated the angular distribution at the intensity of 2.3×10^{18} W/cm². This is in well consistent with the generation mechanism of surface fast electrons. For lower laser intensity, vacuum heating [14] or $J \times B$ heating [15] do not dominate the generation of fast electrons, which consequently results in a weaker magnetic field along the target surface. While with the increase of laser intensity, the two mechanisms gradually play a major role in the generation of fast electrons. Thus, a stronger quasistatic magnetic field is generated along the target surface. Combined with the electrostatic field, more electrons are confined along the target surface, which leads to an enhancement of surface electron current and the magnetic field.

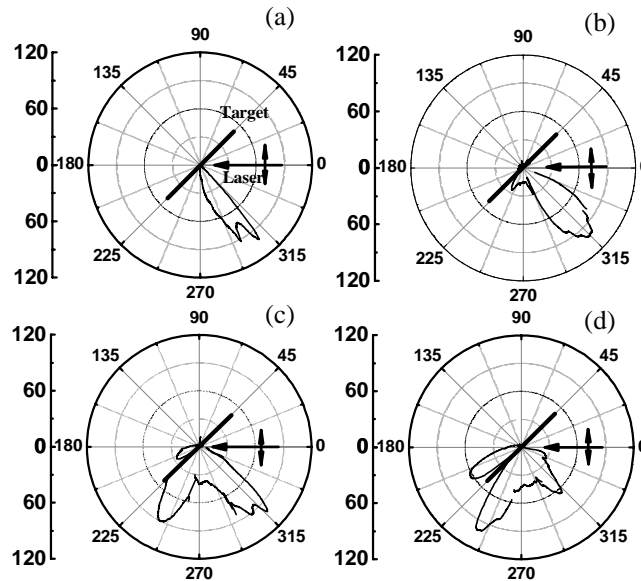


Fig. 3. Angular distribution of the fast electrons with energies larger than 550 keV for the laser intensity of (a) 6×10^{16} W/cm², (b) 7×10^{17} W/cm², (c) 1.5×10^{18} W/cm² and (d) 2.3×10^{18} W/cm². The laser is incident from the right to the left at an angle of 45°.

The relative fractions of the fast electrons emitted close to the front surface, $f_{suf} = N_{suf}/N_{tot}$, and that in the normal direction, $f_{nor} = N_{nor}/N_{tot}$, where N_{suf} is the count of fast electrons close to the front surface, N_{nor} is the count in the normal direction, and N_{tot} is the count of total electrons in both sides of the target, are shown in Fig. 4(a). As the laser intensity is increased, f_{suf} increases, while f_{nor} decreases [Note the absolute numbers of the two groups of electrons increase with the laser intensity. See Fig. 4(b)]. The fast electrons close to the front target surface gradually dominate the angular distribution of the fast electrons for higher laser

intensities. It should be pointed out that the two fractions do not add up to 100 % due to the electrons emitted in the other directions, for example, those in the rear of target, are not shown.

Since the total emitted counts, N_{tot} , of fast electrons increase with the laser intensity, we also compare the absolute counts of the $E > 550$ keV fast electrons emitted close to the front surfaces and that in the target normal direction versus the laser intensities. This is shown in Fig. 4(b). The errors come from the shot-to-shot fluctuations. Each can be fitted with an exponential function,

$$N \sim I_{17}^{0.8} \quad \text{for the electrons in the normal direction,}$$

and
$$N \sim I_{17}^{2.1} \quad \text{for the electrons close to the front surface,}$$

where N is the electron count and I_{17} the laser intensity in 10^{17} W/cm^2 . One can see the counts for both directions increase with the laser intensity. However, the electron count emitted close to the front surface increases much faster than that in the normal direction.

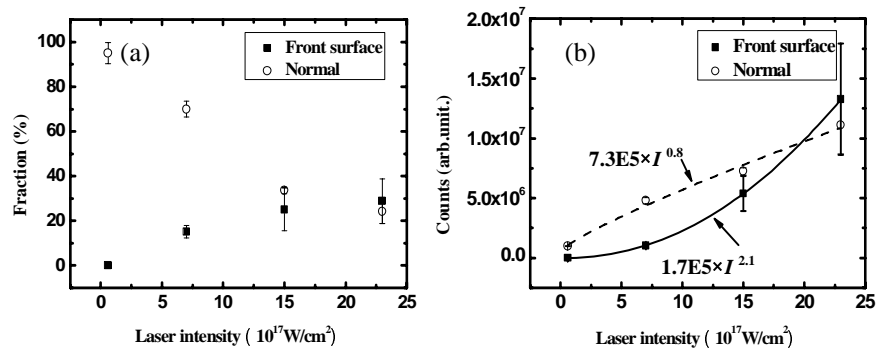


Fig. 4. Fractions (a) and Counts (b) of the fast electrons in the normal (open-circle) and close to the front surface directions (solid square) relative to the total in the whole measured angle range versus the laser intensity. The errors come from the shot-to-shot fluctuations.

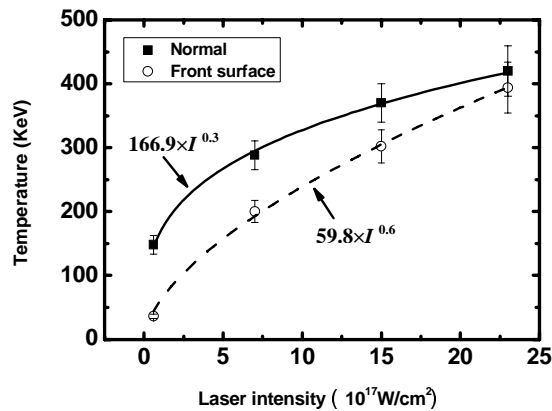


Fig. 5. Temperatures of the fast electrons in the normal (open-circle) and close to the front surface directions (solid square) versus the laser intensity.

The signal intensity on each layer of IP roughly corresponds to the energy deposit by the fast electrons with different energy ranges. Therefore, the spectra of the fast electrons can be estimated. Figure 5 shows the estimated electron temperatures for different laser intensities. Both the temperatures of the fast electrons close to the front surface and those in the normal direction increase with the laser intensities. The electron temperatures are scaled as,

$$T_h \sim I_{17}^{0.3} \quad \text{for the electrons in the normal direction,}$$

and
$$T_h \sim I_{17}^{0.6} \quad \text{for the electrons close to the front surface,}$$

if fitted by exponential distribution, where T_h is the fast electron temperature. The fast electron temperatures close to the front surface increase faster than that in the target normal direction again.

4. Conclusion

The characteristics of the fast electrons close to the front target surface in the interaction of *p*-polarization femtosecond laser pulses with foil targets have been investigated at the laser intensities ranging from 6×10^{16} W/cm² to 2.3×10^{18} W/cm². The fast electrons along the front target surface were observed only for higher laser intensity. Our observation of the more rapid increase of the count, fraction, and the temperature of the fast electrons beam close to the target surface than that in the normal direction with the increase of the laser intensity indicates that the electron acceleration along the front surface is much effective. Similar electron acceleration along the target surface has been proposed to produce high energy electrons using solid capillary targets recently [21].

Acknowledgments

We gratefully thank M. Chen, Dr. Y. Y. Ma and Dr. Q. L. Dong for helpful and fruitful discussion. This work was supported by the National Natural Science Foundation of China (Grant No: 10675164, 60621063, 10575129, 10335020, 10425416 and 10390161.), the National High-Tech ICF program, and National Basic Research Program of China (973 Program) (Grant No. 2007CB815100).